

# SeFAR: Semi-supervised Fine-grained Action Recognition with Temporal Perturbation and Learning Stabilization

Yongle Huang<sup>1,2\*</sup>, Haodong Chen<sup>1,2\*</sup>, Zhenbang Xu<sup>1</sup>, Zihan Jia<sup>3</sup>, Haozhou Sun<sup>4</sup>, Dian Shao<sup>1†</sup>

<sup>1</sup>Unmanned System Research Institute, Northwestern Polytechnical University, Xi'an, China

<sup>2</sup>School of Automation, Northwestern Polytechnical University, Xi'an, China

<sup>3</sup>School of Computer Science, Northwestern Polytechnical University, Xi'an, China

<sup>4</sup>School of Software, Northwestern Polytechnical University, Xi'an, China  
{yonglehuang, chd}@mail.nwpu.edu.cn, shaodian@nwpu.edu.cn

## Abstract

Human action understanding is crucial for the advancement of multimodal systems. While recent developments, driven by powerful large language models (LLMs), aim to be *general* enough to cover a wide range of categories, they often overlook the need for more *specific* capabilities. In this work, we address the more challenging task of Fine-grained Action Recognition (FAR), which focuses on detailed semantic labels within shorter temporal duration (e.g., “salto backward tucked with 1 turn”). Given the high costs of annotating fine-grained labels and the substantial data needed for fine-tuning LLMs, we propose to adopt semi-supervised learning (SSL). Our framework, **SeFAR**, incorporates several innovative designs to tackle these challenges. Specifically, to capture sufficient visual details, we construct *Dual-level temporal elements* as more effective representations, based on which we design a new strong augmentation strategy for the Teacher-Student learning paradigm through involving *moderate temporal perturbation*. Furthermore, to handle the high uncertainty within the teacher model’s predictions for FAR, we propose the *Adaptive Regulation* to stabilize the learning process. Experiments show that SeFAR achieves state-of-the-art performance on two FAR datasets, FineGym and FineDiving, across various data scopes. It also outperforms other semi-supervised methods on two classical coarse-grained datasets, UCF101 and HMDB51. Further analysis and ablation studies validate the effectiveness of our designs. Additionally, we show that the features extracted by our SeFAR could largely promote the ability of multimodal foundation models to understand fine-grained and domain-specific semantics. *Code & Datasets*: <https://github.com/KyleHuang9/SeFAR>.

## Introduction

Understanding videos has attracted increasing attention as videos contain vivid visual information and rich temporal dynamics absent in text and images. In the past year, we have seen remarkable progress in multimodal large language models (MLLMs) (Chen et al. 2023; Li et al. 2024, 2023b; Lin et al. 2023), aiming at acquiring more general and comprehensive abilities. However, as pointed out by recent studies (Zhao et al. 2024; Yuan et al. 2023), chasing generality

\*These authors contributed equally.

†Corresponding Author

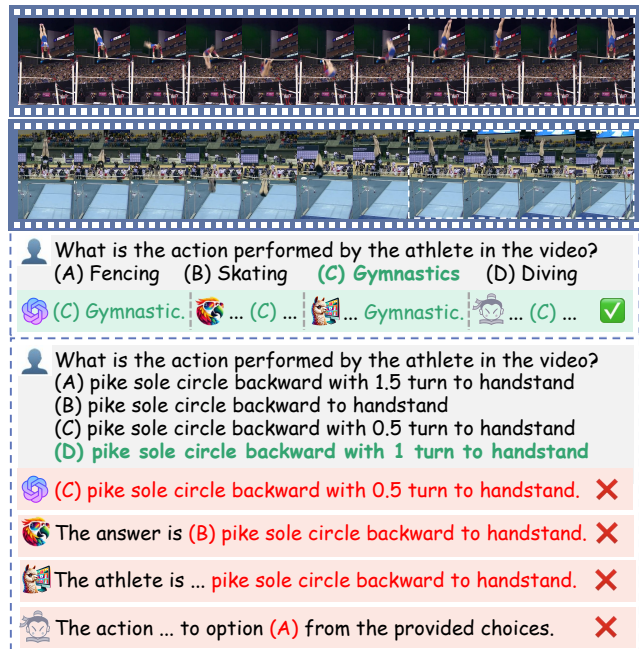


Figure 1: **Fine-grained Action Instances.** The two samples are drawn from the FineGym (Shao et al. 2020a) dataset, specifically the “pike sole circle backward with 0.5 turn to handstand” at the top and the “... 1 turn ...” at the bottom. We further test popular MLLMs on the bottom instance for both coarse-grained and fine-grained: GPT-4V (OpenAI 2024), VideoChat2 (Li et al. 2024), VideoLLaVA (Lin et al. 2023), and InternLM-XComposer-2.5 (Zhang et al. 2024).

may sacrifice some task-specific performance, which motivates us to delve into a perpendicular direction: focus on more *specific* tasks to promote the fine-grained understanding ability of models.

Specifically, we focus on Fine-grained Action Recognition (FAR), a challenging human-centric video understanding task. To explain, classical action recognition (Xiong et al. 2021; Xiao et al. 2022; Dave et al. 2023; Xing et al. 2023) only demands the model to provide relatively coarse-grained category such as “gymnastics”, while FAR aims to provide more detailed, specific, and semantically accurate descriptions as “pike sole circle backward with 0.5 turn to

*handstand*”. To demonstrate the difficulty of this task, we evaluate four powerful MLLMs (OpenAI 2024; Li et al. 2024; Lin et al. 2023; Zhang et al. 2024), as shown in Fig. 1. Unfortunately, they all fail to correctly recognize the fine-grained semantics of the given action. In such a sense, FAR holds significance in further enhancing the capability of MLLM (Driess et al. 2023; Vemprala et al. 2024), especially in application scenes requiring more accurate and professional information.

However, limited research on FAR not only owes to its higher demands for method design but also the dataset construction (Shao et al. 2020a; Xu et al. 2022a). For example, providing annotations such as “5237D with 3.5 twists” (Xu et al. 2022a) requires adequate expert knowledge, huge annotation time, and large checking efforts to ensure the quality (Shao et al. 2020a). This leads to the scarcity of fine-grained labels and makes it difficult to directly re-train or fine-tune large models with huge annotated data. Keep this in mind, we further adopt the semi-supervised learning (SSL) setting, where only a small percentage of labeled data is needed (Zhu 2005). Consequently, targeting semi-supervised FAR, besides those intrinsic challenges from both sides, we have to tackle intractable *new challenges* that emerged when combined. Specifically, FAR needs enough visual details, effective information aggregation, and a comprehensive understanding of temporal dynamics (Shao et al. 2020a; Xu et al. 2022a; Li et al. 2022; Tang et al. 2023). For SSL, the core is to equip the unlabeled data with stable and reasonable supervision (e.g., pseudo-labels) (Sohn et al. 2020; Zhu 2005; Kurakin et al. 2020). However, when training a semi-supervised FAR model, the generated pseudo-labels may not be reliable, since FAR is rather challenging, making the whole learning process easily collapse.

In this paper, we propose a novel framework, **SeFAR**, to address the above challenges. Due to the semi-supervised setting, SeFAR is developed based on the FixMatch (Sohn et al. 2020) SSL paradigm, including the weak-to-strong consistency regularization and the Teacher-Student setup, as shown in Fig. 2. Moreover, there are also delicately designed strategies and modules incorporated in SeFAR: ❶ First, to effectively mine adequate and useful data for FAR, a *dual-level information modeling* strategy is proposed. This process combines both fine-grained temporal elements with the temporal context to effectively capture multi-granular temporal information, enhancing the ability to discriminate subtle actions in the video. ❷ Then, to construct weak-strong contrast data pairs more tailored for FAR which differs from the traditional spatial-only augmentations (Yun et al. 2019; DeVries 2017; Kurakin et al. 2020), we highlight the significance of temporal dynamics and design a new strong augmentation strategy. Specifically, we introduce *moderate temporal perturbation* into the fine-grained temporal elements achieved previously, while keeping the temporal order of context element. ❸ Moreover, in order to provide reliable pseudo-labels for unlabeled data even when the Teacher model suffers from unstable predictions, we design an *Adaptive Regulation* to stabilize the training process by calculating coefficients to adjust the losses. In addition, to directly tackle the problems outlined in Fig. 1, we adhere to the stan-

dard MLLM framework, which includes a vision encoder, a language encoder, and an alignment adapter. By incorporating our SeFAR model as an innovative video encoder, we observe that all MLLMs perform better on FAR, as shown in Tab. 5.

To summarize, our contributions are as follows:

- To the best of our knowledge, this is the first work to explore the highly challenging task of **Semi-supervised Fine-grained Action Recognition** and an effective framework **SeFAR** is proposed for this purpose, which is based on the FixMatch paradigm but incorporates a new augmentation strategy to form the weak-to-strong data pairs;
- Moreover, SeFAR incorporates several innovative designs to address specific challenges, including the dual-level temporal elements modeling, careful involvement of moderate temporal perturbation, as well as the adaptive regulation for a steady learning process;
- SeFAR achieves state-of-the-art performance on both fine-grained (FineGym, FineDiving) and coarse-grained action recognition datasets (UCF101, HMDB51), demonstrating its effectiveness. Additional analysis shows that SeFAR could also serve as a powerful visual encoder to assist current MLLMs in domain-specific scenes.

## Related Work

**Fine-grained Action Recognition (FAR).** FAR aims to differentiate between similar human actions at a finer semantic granularity (e.g., “switch leap with 0.5 turns” vs. “split jump with 1 turn”), while coarse-grained actions (Zhou et al. 2018; Carreira and Zisserman 2017; Xu et al. 2022b; Yang et al. 2020; Wang et al. 2018), stop at the granularity of “gymnastics”. To achieve this, abundant and subtle motion details are extremely desired (Shao et al. 2020a). There are several pioneer works (Li et al. 2022; Leong et al. 2022, 2021; Tang et al. 2023; Hong et al. 2021; Wang et al. 2021) to tackle the problem of FAR. However, they have predominantly focused on fully supervised or few-shot learning. Among them, LCDC (Mac et al. 2019) capture local spatio-temporal features, HAAN (Li, He, and Xu 2022) use hierarchical modeling with atomic actions and visual concepts, while M<sup>3</sup>Net (Tang et al. 2023) implement multi-view encoding, matching, and fusion. Distinct from the above works, we propose to address a more challenging task and propose the first semi-supervised FAR framework, SeFAR, integrating with the *dual-level temporal elements modeling*, which tackles the subtle inter-class differences but also contends with limited annotations.

**Data Augmentation in Semi-supervised Learning (SSL).** Data augmentation plays an essential role in SSL, serving as one of the two core components of the FixMatch (Sohn et al. 2020)-based paradigm, specifically *consistency regularization* achieved through both strong and weak data augmentation. This has been previously demonstrated. For instance, (Xie et al. 2020) emphasizes that a robust model should withstand variations in input examples or hidden states. However, most existing semi-supervised video action recognition studies (Xu et al. 2022b; Xiong et al. 2021; Xiao

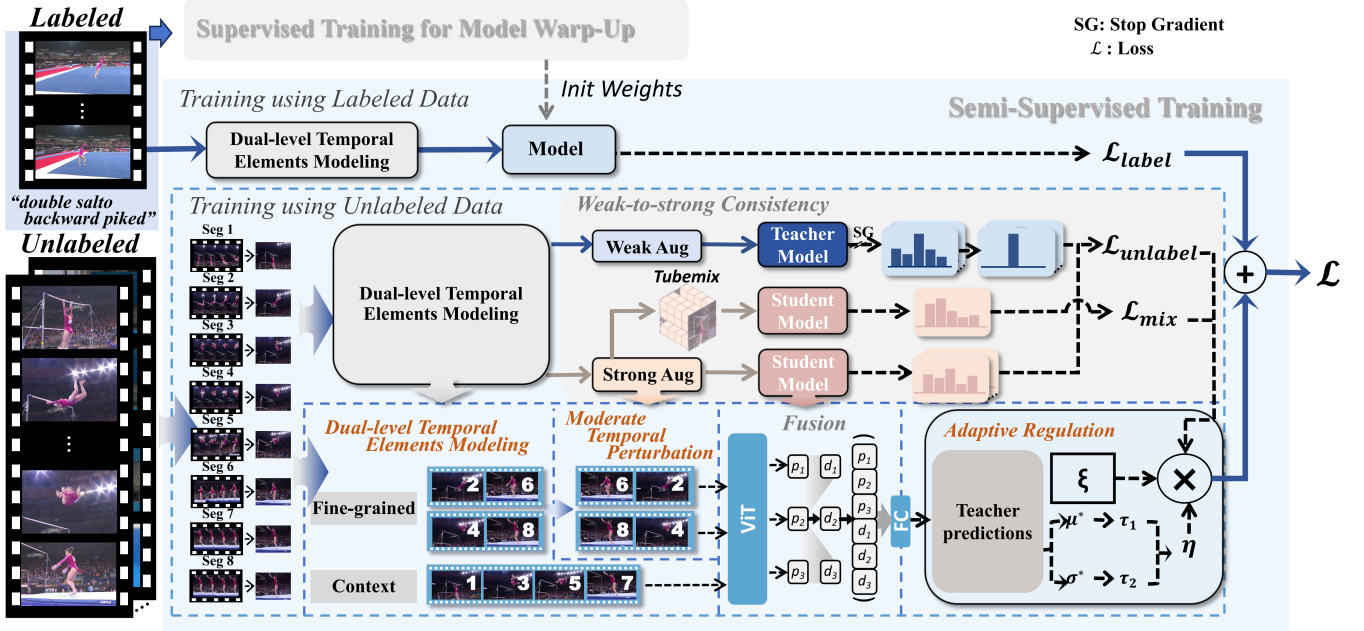


Figure 2: **Overview of SeFAR pipeline.** We target Semi-supervised FAR, assuming most input samples are unlabeled. During unsupervised learning, SeFAR adopts *dual-level temporal elements modeling* and performs augmentation in two manners (‘Weak’ vs. ‘Strong’). Strongly augmented/distorted samples by *moderate temporal perturbation* are used by the student model, while the teacher model offers pseudo-labels based on weakly augmented samples. Consistency is enforced through loss minimization ( $\mathcal{L}_{un}$ ). The unsupervised loss is further adjusted by our proposed *Adaptive Regulation*. The framework is trained with a weighted combination of supervised  $\mathcal{L}_{sup}$  and unsupervised  $\mathcal{L}_{un}$  losses.

et al. 2022; Dave et al. 2023) focus primarily on spatial augmentations achieved through image-based strategies (e.g., Cutmix (Yun et al. 2019), Cutout (DeVries 2017), or their variants (Kurakin et al. 2020; Cubuk et al. 2020)). We argue that temporal augmentation is equally important inspired by (Xing et al. 2023), especially in FAR, as spatial augmentations can often disrupt critical information within actions. To address this, we design a new temporal augmentation strategy, *moderate temporal perturbation*. Furthermore, to maintain stability in the *pseudo-labeling* process, another core component of the FixMatch-based paradigm, we have developed the *Adaptive Regulation* during training.

## Methodology

To tackle the challenging task of semi-supervised fine-grained action recognition, we propose the SeFAR framework, and the complete pipeline is shown in Fig. 2. Before delving into specific details, we first elaborate on the preliminaries about semi-supervised learning, especially the FixMatch (Sohn et al. 2020) paradigm.

### Preliminaries

□ **Teacher vs. Student Model.** A line of SSL frameworks adopts the Teacher-Student setting, where the *Teacher* provides pseudo-labels to supervise the *Student* model. Instead of directly sharing weights between teacher and student models (Sohn et al. 2020), we adopt an average of consecutive student models to obtain a “Mean teacher”, whose effectiveness has been verified (Tarvainen and Valpola 2017). Formally, at a given time step, the weights of the *Teacher*

model,  $\theta_t$ , is updated as an exponential moving average of the student weights  $\theta_s$ :

$$\theta_t \leftarrow \omega \theta_s + (1 - \omega) \theta_t. \quad (1)$$

As pointed out in (Xing et al. 2023), such EMA-Teacher is more suitable and stable for human action recognition.

□ **Weak vs. Strong Augmentation.** One core component within FixMatch (Sohn et al. 2020) is the construction of contrastive data pairs to facilitate consistency regularization. This involves the incorporation of both strong and weak augmentations, wherein the term “*augmentation*” here means “*distortion*” rather than “*enhancement*”, contrary to intuition. Specifically, strong augmentation ( $\mathcal{A}_{strong}$ ) usually causes significant perturbation to the original data and thus serves as the input for the Student model, while the  $\mathcal{A}_{weak}$  produces moderately distorted data samples for the Teacher model to derive better predictions, as demonstrated in the center part of Fig. 2.

□ **Learning by Labeled vs. Unlabeled Data.** In the SSL setting, only a small portion of data is annotated, denoted by  $\{x_i, y_i\}_{i=1}^{\mathcal{B}_l}$ . The left  $\mathcal{B}_u$  samples,  $\{x_j\}_{j=1}^{\mathcal{B}_u}$ , are all unlabeled. Usually the labeling ratio  $\alpha = \frac{\mathcal{B}_l}{\mathcal{B}_l + \mathcal{B}_u}$  is small (e.g., 0.1). Learning based on the labeled data is straightforward by minimizing the cross-entropy loss between model predictions  $Pred(x_i)$  and labels  $y_i$ :

$$\mathcal{L}_{sup} = \frac{1}{\mathcal{B}_l} \sum_{i=1}^{\mathcal{B}_l} \mathcal{H}(y_i, Pred(x_i)). \quad (2)$$

However, for the unlabeled data  $x_j$ , there is no supervision.

To solve this, we generate pseudo-labels from the Teacher model predictions  $\mathcal{F}^T$ , and then calculate the unsupervised loss as follows:

$$\hat{y}_j = \max(\mathcal{F}_t(\mathcal{A}_{weak}(x_j)),$$

$$\mathcal{L}_{un} = \frac{1}{B_u} \sum_{j=1}^{B_u} \mathbf{1}(\hat{y}_j > \tau) \mathcal{H}(\hat{y}_j, \mathcal{F}_s(\mathcal{A}_{strong}(x_j))), \quad (3)$$

where  $\tau$  is the predefined threshold for confidence scores and  $\mathbf{1}$  denotes the indicator function. The whole pipeline is trained using both losses, weighted by hyperparameters,

$$\mathcal{L} = \gamma_1 \mathcal{L}_{sup} + \gamma_2 \mathcal{L}_{un}. \quad (4)$$

## The SeFAR Framework

In this work, we focus on the task of Fine-grained Action Recognition (FAR) in the Semi-Supervised Learning (SSL) setting. This new task brings unprecedented challenges, including: ❶ How to mine abundant and detailed visual information for differentiating subtle differences between fine-grained actions? ❷ How to adapt the original SSL strategies, e.g., consistency regularization, to fit the ‘‘temporal-matters’’ FAR task? ❸ How to deal with the unstable pseudo-labels since the model hesitates between appearance-similar action samples? In the following paragraphs, we will introduce specific designs to address the above challenges.

○ **Dual-level Temporal Elements.** Given a fine-grained action video with  $N$  frames, we first trim it into  $K$  segments (Wang et al. 2016), and randomly sample one frame in each segment, obtaining a frame sequence  $\{f_1, \dots, f_K\}$  to represent the video. Since in FAR, the high similarity is shared in large parts of visual content (e.g., scenes, objects), models are usually required to perceive subtle changes and abundant details for accurate discrimination. To achieve this, we propose to construct several small temporal elements  $p_i$ , where ‘‘small’’ means the size  $L$  (i.e., the number of containing frames) of  $p_i$  is moderate. Intuitively, a small value of  $L$  could help the model focus on quick and subtle changes, since details are usually missed when going through too many frames. Given  $K$  frames, the sampling step is  $\lfloor \frac{K}{L} \rfloor$ . After sampling  $M$  times, we could get a set of temporal elements with the same temporal lengths, denoted by:

$$\{p_i\}_{i=1}^M, \quad |p_i| = L. \quad (5)$$

Besides these temporally fine-grained elements, we also propose to obtain a context element  $p^{\text{context}}$  to encode long-term information and macro temporal dynamics.  $p^{\text{context}}$  is composed of more frames, usually two times more than the fine-grained temporal elements  $p_i$ . Such dual-level information modeling ensures that multi-granular information is preserved. As a result, we obtain an effective representation of the input video, denoted by  $\{p_1, \dots, p_M, p^{\text{context}}\}$ .

○ **Perturbation of Fine-grained Temporal Elements.** Adopting the FixMatch (Sohn et al. 2020) based semi-supervised learning setting, one key problem is ‘‘how to form the weak-to-strong augmentation pair for consistency regularization’’. For weak augmentation, we could use random horizontal flipping or random scaling, since it largely preserves both spatial and temporal original information.

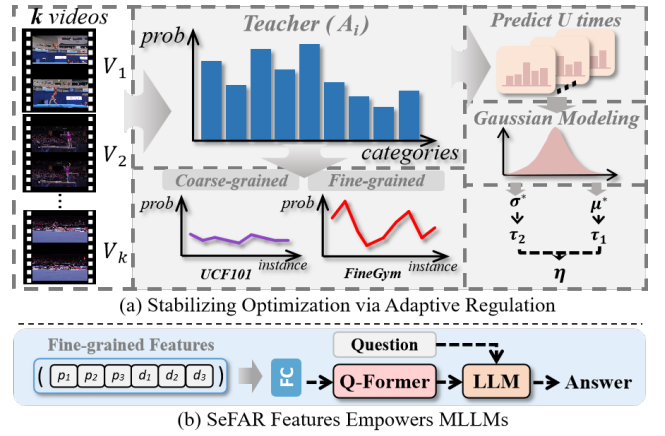


Figure 3: **(a)** For  $K$  unlabeled videos, the Teacher model predicts each video multiple times to capture the distribution of predictions, which shows less variability on coarse-grained data and more on fine-grained data. An adaptive coefficient  $\eta$  is calculated from the mean and variance of the distribution to stabilize training. **(b)** MLLM construction pipeline with SeFAR’s fine-grained features.

Unfortunately, as pointed out in (Xing et al. 2023), strong augmentation designed for images is insufficient for video tasks, since it fully ignores the temporal dynamics evolving in videos. For the challenging FAR task, temporal variations are even more crucial and require the extreme attention of the model. Therefore, to design more effective strong augmentation strategy  $\mathcal{A}_{strong}$  for FAR, we emphasize the following core insights: ❶ the proposed  $\mathcal{A}_{strong}$  should make perturbations to the most crucial part of the data that we want the model to attend to (Sohn et al. 2020; Xie et al. 2020; Kurakin et al. 2020); ❷ Employing  $\mathcal{A}_{strong}$  should not affect the semantic distinctiveness of action categories.

Therefore, combing with the above dual-level temporal modeling strategy, we propose a new strong augmentation operation through introducing temporal perturbation  $\psi$  into the fine-grained temporal elements  $\{p_i\}$ . We experiment with different implementations of  $\psi$ , and the final choice is simple but effective: *reversing the frame order*. Specifically, we have:

$$\mathcal{A}_{strong}(\{p_i\}_{i=1}^M) = \{\overleftarrow{p_i}\}_{i=1}^M, \quad \overleftarrow{p_i} = \psi(p_i) \quad (6)$$

Note that for the temporal context element  $p^{\text{context}}$ , the temporal order is preserved, which ensures the temporal directionality to be inherent in actions (e.g., ‘‘giant circle backward’’ vs. ‘‘giant circle forward’’, etc.), as shown in the bottom-left of Fig. 2. Our augmentation strategy introduces moderate temporal perturbation compared with total shuffling, and it also outperforms previous strategies, e.g., temporal warping (Xing et al. 2023), as shown in Tab. 4.

○ **Stabilizing Optimization via Adaptive Regulation.** As mentioned, due to the challenging intrinsic of FAR, models usually swayed precariously between categories with subtle differences. During experiments, the greater the uncertainty of the model’s predictions, the less reliable the model’s predictions are. Such unstable predictions of the teacher model will result in ambivalent and invalid pseudo-

Table 1: **Comparison with state-of-the-art semi-supervised action recognition methods on fine-grained datasets.** We employ SeFAR with a sampling combination of  $\{2-2-4\}$ . The primary evaluation metric is top-1 accuracy. In this table, ‘‘V’’ within ‘‘Input’’ denotes RGB video, while ‘‘G’’ represents temporal gradients. ‘‘ImgNet’’ indicates the utilization of models pre-trained on ImageNet (Russakovsky et al. 2015), while ‘‘#F’’ signifies the number of input frames. The labeling rates of the data are indicated by ‘‘5%’’, ‘‘10%’’, and ‘‘20%’’ in the datasets. The best results are highlighted in **Bold**, and the second-best Underlined.

Method	Backbone	Input	ImgNet	Params	#F	Epoch	Gym99		Gym288		Diving	
							5%	10%	5%	10%	5%	10%
MemDPC (ECCV’20) (Han, Xie, and Zisserman 2020)	3D-ResNet-18	V	✗	15.4M	16	500	10.8	24.1	14.5	21.3	54.3	62.0
LTG (CVPR’22) (Xiao et al. 2022)	3D-ResNet-18	VG	✗	68.3M	8	180	34.3	45.8	16.2	38.7	59.8	64.3
SVFormer (CVPR’23) (Xing et al. 2023)	ViT-B	V	✓	121.4M	8	30	31.4	47.9	21.3	39.6	59.1	70.8
SeFAR-S (Ours)	VIT-S	V	✓	31.2M	8	30	<u>36.7</u>	<u>56.3</u>	<u>27.8</u>	<u>46.9</u>	<u>72.2</u>	<u>78.4</u>
SeFAR-B (Ours)	VIT-B	V	✓	122.1M	8	30	<b>39.0</b>	<b>56.9</b>	<b>28.3</b>	<b>48.1</b>	<b>72.8</b>	<b>80.9</b>

(a) Results of elements across all events.

Method	UB		FX		10m	
	10%	20%	10%	20%	10%	20%
MemDPC	20.7	19.1	13.8	15.9	65.4	71.2
LTG	50.5	60.5	19.6	21.6	75.2	83.5
SVFormer	52.9	66.8	20.1	28.8	73.8	85.9
SeFAR-S (Ours)	56.9	73.8	23.8	42.9	85.5	94.0
SeFAR-B (Ours)	<b>58.5</b>	<b>75.5</b>	<b>27.6</b>	<b>44.2</b>	<b>87.4</b>	<b>94.6</b>

(b) Results of elements within an event.

Method	UB-S1		FX-S1		5253B	
	10%	20%	10%	20%	10%	20%
MemDPC	17.2	21.1	15.4	20.1	82.2	89.5
LTG	21.3	29.7	14.6	19.3	64.6	76.9
SVFormer	28.9	47.3	18.8	22.5	86.6	90.1
SeFAR-S (Ours)	36.6	55.3	19.2	25.5	96.4	97.3
SeFAR-B (Ours)	<b>37.1</b>	<b>56.8</b>	<b>20.1</b>	<b>26.5</b>	<b>97.0</b>	<b>97.8</b>

(c) Results of elements within a set.

labels for the student, making the whole learning process suffer. To solve this, we first let the *Teacher* model generate predictions  $U$  times ( $U$  is set to 10 in experiments) for a given unlabeled video, and these predictions may vary largely. Then, based on these, we calculate the mean prediction confidence and standard deviation for each category. For the  $i^{th}$  prediction, the predicted probability across all categories constitutes a probability distribution. From this distribution, we can obtain the maximum prediction confidence value  $\mu^i$  and calculate its standard deviation  $\sigma^i$ . We select the highest confidence value  $\mu^* = \max(\mu^i)$ , along with its corresponding standard deviation  $\sigma^*$  (see Fig. 5).

Based on such  $\mu^*$  and  $\sigma^*$ , we propose to calculate the dynamic coefficients  $\tau_1$  and  $\tau_2$  to obtain  $\eta$ , which is further used for adjusting losses derived from unlabeled samples:

$$\begin{aligned} \tau_1 &= \text{sigmoid}(e^{\mu^*} - e), \\ \tau_2 &= (\text{sigmoid}(\frac{1}{\beta\sigma^* + \epsilon}) - 0.5), \end{aligned} \quad (7)$$

where  $\beta$  is related to the model dropout and  $\epsilon$  is a steady parameter. To elaborate,  $\tau_1$  will increase rapidly as  $\mu^*$  increases, which enhances high-confidence predictions, while on the other hand,  $\tau_2$  suppresses the unstable predictions (*i.e.*, with high standard deviation  $\sigma$ ). The obtained adaptive coefficient  $\eta = \tau_1 \cdot \tau_2$ , is more flexible and beneficial than a predefined hyperparameter. Additionally, for unlabeled data, we also adopt the mixing strategy as in SVFormer (Xing et al. 2023), where the mixture of two unlabeled samples,  $\lambda x_1 + (1 - \lambda)x_2$ , could also serve as input, and the supervision is correspondingly obtained as a mixed version (Details could be found in (Xing et al. 2023)). Here for adjusting  $\mathcal{L}_{mix}$ , we achieve its coefficient in a similar mixed manner, denoted by  $\eta' = \lambda\eta_1 + (1 - \lambda)\eta_2$ , where  $\eta_1, \eta_2$  are individually calculated based on  $x_1$  and  $x_2$ . Finally, the total loss of the whole SeFAR framework is as follows:

$$\mathcal{L} = \mathcal{L}_{sup} + \xi(\eta\mathcal{L}_{un} + \eta'\mathcal{L}_{mix}), \quad (8)$$

where  $\xi = \sin(\frac{n}{M_n})$  is a warmup coefficient calculated using the current epoch number  $n$  and the max epoch  $M_n$ .

○ **SeFAR Empowers MLLMs.** Efforts towards foundation models have led to the development of MLLMs, with vision being the primary modality (Gao et al. 2024). Although shown impressive general capabilities, they may fail in specific and more challenging tasks such as FAR, as illustrated in Fig. 1. This may largely be due to the systematic shortcomings in the visual part as analyzed in (Tong et al. 2024). Given that our SeFAR is designed to be effective for FAR in semi-supervised scenarios, the question: ‘‘*Could SeFAR benefit current MLLMs through providing better visual perception?*’’ The answer is yes as supported by the results in Tab. 5. To elaborate, in line with the typical MLLM framework, a frozen visual encoder is usually combined with a LLM. This setup facilitates multimodal functionality by aligning visual and textual features using an adaptor, *e.g.*, Q-Former (Li et al. 2023a). Given such a setting, we could use the features extracted by SeFAR to replace those provided by the original visual encoder as shown at the bottom of Fig. 5. Similarly, by aligning the visual features with the textual domain and concatenating with text embeddings, we could feed them into the LLM to produce the answers. Results show that SeFAR features could lead to much better results compared to those used in original MLLM settings.

## Experiment

### Experiment Setup

**Datasets and Evaluation.** We perform evaluations on fine-grained datasets Gym99, Gym288 (Shao et al. 2020a), and FineDiving (Xu et al. 2022a), as well as coarse-grained datasets UCF-101 (Soomro 2012) and HMDB-51 (Kuehne et al. 2011), using Top-1 accuracy as metrics. Specifically, FineGym includes hierarchical annotations at three semantic granularity: *events*, *sets*, and *elements*. At the finest level (*elements*), there are two versions of benchmarks, *i.e.*, *gym99*

Table 2: **Comparison with state-of-the-art semi-supervised action recognition methods on coarse-grained datasets.** “V” within “Input” signifies RGB video, “F” indicates optical flow, while “G” denotes temporal gradients.

Method	Backbone	Input	ImgNet	#F	Epoch	UCF-101		HMDB-51		
						1%	5%	10%	40%	50%
MT+SD (WACV’21) (Jing et al. 2021)	3D-ResNet-18	V	✗	16	500	-	31.2	40.7	32.6	35.1
MvPL (ICCV’21) (Xiong et al. 2021)	3D-ResNet-50	VFG	✗	8	600	22.8	41.2	80.5	30.5	33.9
TCLR (CVIU’22) (Dave et al. 2022)	3D-ResNet-18	V	✗	16	1200	26.9	-	66.1	-	-
CMPL (CVPR’22) (Xu et al. 2022b)	R50+R50-1/4	V	✗	8	200	25.1	-	79.1	-	-
LTG (CVPR’22) (Xiao et al. 2022)	3D-ResNet-18	VG	✗	8	180	-	44.8	62.4	46.5	48.4
TimeBalance (CVPR’23) (Dave et al. 2023)	3D-ResNet-50	V	✗	8	250	30.1	53.3	81.1	52.6	53.9
SeFAR (Ours)	ViT-S	V	✗	8	30	35.2	64.1	78.3	55.9	59.2
FixMatch (NeurIPS’20) (Sohn et al. 2020)	SlowFast-R50	V	✓	8	200	16.1	-	55.1	-	-
MemDPC (ECCV’20) (Han, Xie, and Zisserman 2020)	3D-ResNet-18	V	✓	16	500	-	-	44.2	-	-
ActorCM (CVIU’21) (Zou et al. 2023)	R(2+1)D-34	V	✓	8	360	-	45.1	53.0	35.7	39.5
VideoSSL (WACV’21) (Jing et al. 2021)	3D-ResNet-18	V	✓	16	500	-	32.4	42.0	32.7	36.2
TACL (TSVT’22) (Tong, Tang, and Wang 2023)	3D-ResNet-50	V	✓	16	200	-	35.6	55.6	38.7	40.2
L2A (ECCV’22) (Gowda et al. 2022)	3D-ResNet-18	V	✓	8	400	-	-	60.1	42.1	46.3
SVFormer-S (CVPR’23) (Xing et al. 2023)	ViT-S	V	✓	8	30	31.4	-	79.1	56.2	58.2
SVFormer-B (CVPR’23) (Xing et al. 2023)	ViT-B	V	✓	8	30	46.1	-	84.6	59.9	64.3
SeFAR (Ours)	ViT-S	V	✓	8	30	46.0	73.2	84.3	58.5	62.9
SeFAR (Ours)	ViT-B	V	✓	8	30	<b>50.3</b>	<b>77.6</b>	<b>87.0</b>	<b>61.5</b>	<b>65.7</b>

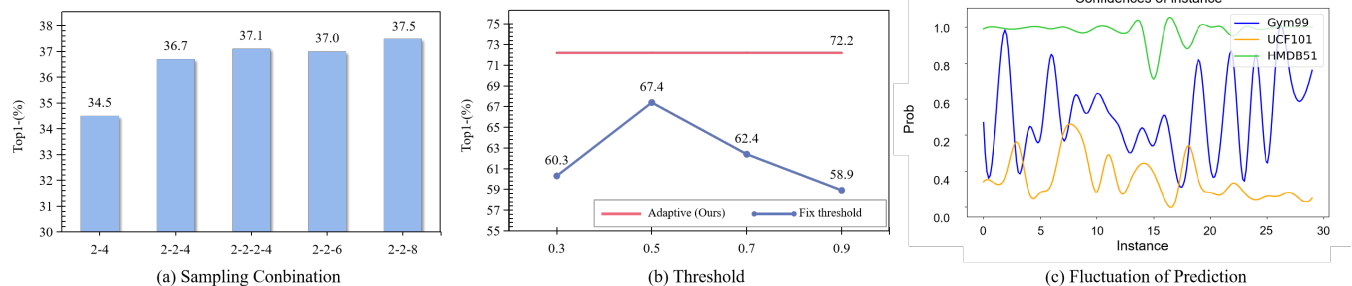


Figure 4: **Ablation Studies.** We compare SeFAR-B with different sampling combinations on Gym-99 5%, as illustrated on the **left**. We also contrast fixed threshold methods with our Adaptive Regulation strategy on FineDiving 5% in the **middle**. On the **right** side, we demonstrate the fluctuation of predictions made by the Teacher model across different datasets.

and *gym288*, with 99 and 288 categories, respectively. Note that all the experiments on FineGym are performed at the element level, but within different scopes. FineDiving is a diving dataset comprising 3000 annotated clips with timestamps, encompassing 52 *action* types, 29 *sub-action* types, and 23 difficulty levels.

**Baselines.** We employ the ViT (Dosovitskiy 2020) extended model TimeSformer (Bertasius, Wang, and Torresani 2021) as the backbone. The choice of hyperparameters remains as original. We instantiate the SeFAR-S model based on ViT-Small, with the number of total parameters comparable to most previous Conv-based methods (Han, Xie, and Zisserman 2020; Xiong et al. 2021; Xu et al. 2022b; Xiao et al. 2022; Tong, Tang, and Wang 2023; Gowda et al. 2022; Dave et al. 2023). Moreover, we implement the SeFAR-B model based on ViT-B, with more parameters. We configure the sampling combination by default as  $\{2 - 2 - 4\}$  for SeFAR, as commonly used 8-frame input.

**Implementation Details.** We employ our SeFAR using PyTorch, with input video frames resized and cropped to  $224 \times 224$  pixels. We adopt the SGD optimizer and employ a learning rate of 0.005, momentum of 0.9, and weight decay of 0.001. The weights in Eq.4 are set as:  $\lambda_1 = \lambda_2 = 2$ .

## Main Results

The main quantitative results on the two fine-grained action recognition datasets, *i.e.*, FineGym and FineDiving, are demonstrated in Tab. 1. We evaluate all the methods at different semantic granularities. Specifically, we first conduct experiments on Gym99 and Gym288. Then, by narrowing the semantic granularity, we focus on those element-level categories belonging to a specific event. For instance, in Gym99, 25 classes belong to Uneven-bars (UB), while 35 classes are from Floor-exercise (FX). Further, we delve into the finer granularity, collecting sampling within that same set in the same event. Here we get all the circles in UB-set1 (UB-S1) and all the jumps in FX-set1 (FX-S1) for evaluation. We can observe that on both the FineGym and FineDiving, SeFAR-S significantly outperforms previous *open-sourced* semi-supervised action recognition methods across all semantic granularities with moderate parameters. Additionally, when increasing the parameters comparative with SVFormer (Xing et al. 2023), the larger model, SeFAR-B, performs even better. Both SeFAR-S and SeFAR-B display the effectiveness of our proposed SeFAR framework for addressing the challenging task.

Moreover, to further inspect the effectiveness and robustness of SeFAR, we conducted experiments on two classical coarse-grained action recognition datasets, UCF-101 and

Table 3: **Ablations of different components with SeFAR**, where ✓ means “w/”. To adhere to the principle of consistency regularization in SSL, we employ strong augmentation consistent with SVFormer (Xing et al. 2023), *i.e.*, temporal warping, once our Mod-Perturb is eliminated.

Dual-Ele	Mod-Perturb	Ada-Reg	Gym99	Gym288	Diving
✗	✗	✗	32.6	22.7	60.4
✓	✗	✗	34.8	25.4	64.6
✓	✓	✗	35.9	26.6	67.4
✓	✓	✓	<b>36.7</b>	<b>27.8</b>	<b>72.2</b>

Table 4: **Ablation of different temporal augmentations. S and O** denote the Speed- and Order-focused.

Perturbation	S/O	Gym99	Gym288	Diving	G.-New	Sth.-Sth.
Spatial-only		34.2	24.4	67.9	45.6	39.4
Slow (T-Drop)	S	35.6	25.2	68.6	45.0	41.2
All shuffle	O	35.2	26.3	69.0	45.5	41.9
Local-shuffle	O	36.4	27.6	71.9	45.3	43.3
Warping	O	35.9	24.7	68.2	44.8	40.8
T-Half	O	36.0	24.8	68.4	44.8	42.1
All reverse	O	36.3	27.3	71.2	45.9	42.7
Mod-Perturb	O	<b>36.7</b>	<b>27.8</b>	<b>72.2</b>	<b>46.2</b>	<b>44.9</b>

HMDB-51. As shown in Tab. 2, SeFAR-B achieves approximately 3.3% improvement on UCF101 and approximately 1.7% improvement on HMDB51, achieving new state-of-the-art results compared with those competitive baselines.

### Ablation Studies

To achieve an in-depth comprehension of our SeFAR framework, we perform ablation studies on the impact of each component, namely *dual-level temporal elements modeling* (Dual-Ele), *moderate temporal perturbation* (Mod-Perturb) and *Adaptive Regulation* (Ada-Reg), as demonstrated in Tab. 3. Each module contributes significantly as an essential part of SeFAR. Furthermore, we conduct a comprehensive analysis of the designs and choices of each proposed strategy or module. Details can be found as follows.

#### Analysis of Dual-level Temporal Elements Modeling.

We first compare different combinations of sampled elements, each context element has varying temporal lengths, *e.g.*, 4, 6, 8. To facilitate comparison, we fix the length of the temporal fine-grained elements to be 2, consistent with our default setting {2-2-4}. Results are depicted in the left part of Fig. 4. We can find that even with a limited input of only 6 frames, *i.e.*, {2-4}, our proposed SeFAR surpasses the 8-frame input baseline SVFormer (Xing et al. 2023). This observation justifies the capability of our *dual-level temporal elements modeling* to capture abundant information details from video data, contributing to better discerning subtle differences among fine-grained actions. Additionally, it is noteworthy that increasing the number of the fine-grained elements, *i.e.*, {2-2-2-4}, or extending the temporal length of the context element, *i.e.*, {2-2-6} and {2-2-8}, all leads to performance improvements. This is attributed to the fact that more frames entail richer action information.

**Analysis of Moderate Temporal Perturbation.** To better explore the impact of our proposed moderate temporal per-

Table 5: **Ablation of Pre-trained Visual Encoder.** We employ Vicuna-7B (Chiang et al. 2023) as the base LLM, comparing SeFAR’s features with the pre-trained features of commonly used visual encoders in MLLMs further fine-tuned on 5% data (*i.e.*, 🏠: LLaVA, 🌐: VideoChat2, 🗺️: VideoLLaMA, 🎨: VideoChat, and 🎮: VideoLLaVA)

Visual Encoder	MLLM	Gym-QA-99	Gym-QA-288
CLIP-ViT-L/16	🏠, 🌐	37.3	41.0
EVA-CLIP ViT-G/14	🗺️, 🎨	43.7	44.8
ViT-L/14	🎮	44.3	46.0
SeFAR (Ours)	-	<b>49.0</b>	<b>56.2</b>

turbation (Mod-Perturb), we first selected 40 classes of action pairs that are reversing to each other (*e.g.*, “giant circle backward” vs. “giant circle forward”) from FineGym, forming a subset called **Gym-New** (G.-New). As shown in Tab. 4, SeFAR also maintains superior performance even on such actions, as well as on the Something-Something V2 (Sth.-Sth.) dataset (Goyal et al. 2017). Furthermore, we compare our Mod-Perturb with other temporal perturbation strategies in both Speed- and Order-focused (*e.g.*, slow-rate (Singh et al. 2021), temporal warping (Xing et al. 2023), T-Drop and T-Half (Zou et al. 2023)), the results can be found in Tab. 4. We can observe that: 1) Our Mod-Perturb exhibits superior stability and efficacy compared to other temporal augmentations and spatial-only (temporal information well-kept). 2) Spatial-only is less effective in Gym99 but outperforms most temporally augmented in Gym-New. This suggests that preserving accurate temporal information is crucial for more complex datasets, whereas reasonable temporal perturbations can enhance model stability in larger and more diverse datasets, and Mod-Perturb benefits from both.

**Analysis of Adaptive Regulation.** To justify the usefulness of our stabilizing coefficients for adaptive losses, we perform two analyses: ① We compare this strategy with the fixed thresholding strategy widely used in the classical SSL method, the results are displayed in Fig. 4 (b), showing our method is both stable and effective. ② In Fig. 4 (c), We demonstrate the unstable predictions provided by the teacher models for FAR. Specifically, we randomly draw 30 data samples from different datasets, UCF101, HMDB51, and FineGym, for the teacher model to offer predictions. The highly varying predictions on FineGym further justify the motivation of our stabilizing design for FAR.

#### Analysis of SeFAR Features.

To further demonstrate the capability of SeFAR in enhancing MLLMs, we first constructed the **Gym-QA** dataset, which is derived from FineGym and presented in a multiple-choice format as illustrated in Fig. 1. We then selected three widely used MLLM visual encoders, *i.e.*, CLIP-ViT-L/16, EVA-CLIP ViT-G/14, and ViT-L/14). For fair comparisons, we conduct semi-supervised training on these backbones with 5% labeling data from FineGym. Subsequently, we froze the weights of these encoders along with the weights from our 5%-trained SeFAR, and fine-tuned the Q-former using 5% of the annotated data from Gym-QA. As shown in Tab. 5, the SeFAR-empowered LLM significantly outperformed the other MLLM visual encoders on the Gym-QA task. This

also mitigates the challenge of fine-tuning MLLMs in scenarios with low labeling rates.

## Conclusion

In this work, we shed light on a more challenging and specific video understanding task, Semi-supervised Fine-grained Action Recognition (FAR). To tackle the unique challenges that emerged, we propose a new framework, SeFAR, which adopts ideas from the FixMatch setting and possesses innovative components delicately devised for FAR. Specifically, SeFAR is distinguished due to the following designs: 1) *Dual-level temporal elements modeling* is used to mine visual cues more thoroughly and capture rich temporal dynamics better; 2) *Augmentation via moderate temporal perturbation* is to produce temporally strong-distorted samples for weak-to-strong consistency regularization; 3) *Stabilizing Optimization via Adaptive Regulation* is to address the issue of large uncertainty in model predictions. To highlight, SeFAR also demonstrates superior performance in empowering MLLM’s fine-grained visual understanding capability. SeFAR not only outperforms all the baselines largely on two representative FAR datasets, FineGym and FineDiving, but also achieve new state-of-the-art results on classical benchmarks (*i.e.*, UCF101 and HMDB51). Comprehensive analysis and Extensive ablation studies further justify the effectiveness of our framework design.

## Acknowledgments

This work was funded by the National Natural Science Foundation of China (NSFC) under Grant 62306239, and was also supported by National Key Lab of Unmanned Aerial Vehicle Technology under Grant WR202413.

## References

- Bertasius, G.; Wang, H.; and Torresani, L. 2021. Is space-time attention all you need for video understanding? In *ICML*, volume 2, 4.
- Carreira, J.; and Zisserman, A. 2017. Quo vadis, action recognition? a new model and the kinetics dataset. In *proceedings of the IEEE Conference on Computer Vision and Pattern Recognition*, 6299–6308.
- Chen, H.; Huang, H.; Dong, J.; Zheng, M.; and Shao, D. 2024a. Finecliper: Multi-modal fine-grained clip for dynamic facial expression recognition with adapters. In *Proceedings of the 32nd ACM International Conference on Multimedia*, 2301–2310.
- Chen, H.; Huang, Y.; Huang, H.; Ge, X.; and Shao, D. 2024b. GaussianVTON: 3D Human Virtual Try-ON via Multi-Stage Gaussian Splatting Editing with Image Prompting. *arXiv preprint arXiv:2405.07472*.
- Chen, H.; Wang, L.; Yang, H.; and Lim, S.-N. 2024c. Omni-Creator: Self-Supervised Unified Generation with Universal Editing. *arXiv preprint arXiv:2412.02114*.
- Chen, J.; Zhu, D.; Shen, X.; Li, X.; Liu, Z.; Zhang, P.; Krishnamoorthi, R.; Chandra, V.; Xiong, Y.; and Elhoseiny, M. 2023. Minigpt-v2: large language model as a unified interface for vision-language multi-task learning. *arXiv preprint arXiv:2310.09478*.
- Chiang, W.-L.; Li, Z.; Lin, Z.; Sheng, Y.; Wu, Z.; Zhang, H.; Zheng, L.; Zhuang, S.; Zhuang, Y.; Gonzalez, J. E.; et al. 2023. Vicuna: An open-source chatbot impressing gpt-4 with 90%\* chatgpt quality. See <https://vicuna.lmsys.org> (accessed 14 April 2023), 2(3): 6.
- Cubuk, E. D.; Zoph, B.; Shlens, J.; and Le, Q. V. 2020. Randaugment: Practical automated data augmentation with a reduced search space. In *Proceedings of the IEEE/CVF conference on computer vision and pattern recognition workshops*, 702–703.
- Dave, I.; Gupta, R.; Rizve, M. N.; and Shah, M. 2022. TCLR: Temporal contrastive learning for video representation. *Computer Vision and Image Understanding*, 219: 103406.
- Dave, I. R.; Rizve, M. N.; Chen, C.; and Shah, M. 2023. Timebalance: Temporally-invariant and temporally-distinctive video representations for semi-supervised action recognition. In *Proceedings of the IEEE/CVF Conference on Computer Vision and Pattern Recognition*, 2341–2352.
- Dave, I. R.; Rizve, M. N.; and Shah, M. 2025. Finepseudo: improving pseudo-labelling through temporal-alignability for semi-supervised fine-grained action recognition. In *European Conference on Computer Vision*, 389–408. Springer.
- DeVries, T. 2017. Improved Regularization of Convolutional Neural Networks with Cutout. *arXiv preprint arXiv:1708.04552*.
- Dosovitskiy, A. 2020. An image is worth 16x16 words: Transformers for image recognition at scale. *arXiv preprint arXiv:2010.11929*.
- Driess, D.; Xia, F.; Sajjadi, M. S.; Lynch, C.; Chowdhery, A.; Ichter, B.; Wahid, A.; Tompson, J.; Vuong, Q.; Yu, T.; et al. 2023. Palm-e: An embodied multimodal language model. *arXiv preprint arXiv:2303.03378*.
- Gao, P.; Zhang, R.; Liu, C.; Qiu, L.; Huang, S.; Lin, W.; Zhao, S.; Geng, S.; Lin, Z.; Jin, P.; et al. 2024. Sphinx-x: Scaling data and parameters for a family of multi-modal large language models. *arXiv preprint arXiv:2402.05935*.
- Gowda, S. N.; Rohrbach, M.; Keller, F.; and Sevilla-Lara, L. 2022. Learn2augment: learning to composite videos for data augmentation in action recognition. In *European conference on computer vision*, 242–259. Springer.
- Goyal, R.; Ebrahimi Kahou, S.; Michalski, V.; Materzynska, J.; Westphal, S.; Kim, H.; Haenel, V.; Fruend, I.; Yianiilos, P.; Mueller-Freitag, M.; et al. 2017. The” something something” video database for learning and evaluating visual common sense. In *Proceedings of the IEEE international conference on computer vision*, 5842–5850.
- Han, T.; Xie, W.; and Zisserman, A. 2020. Memory-augmented dense predictive coding for video representation learning. In *European conference on computer vision*, 312–329. Springer.



- Hong, J.; Fisher, M.; Gharbi, M.; and Fatahalian, K. 2021. Video pose distillation for few-shot, fine-grained sports action recognition. In *Proceedings of the IEEE/CVF International Conference on Computer Vision*, 9254–9263.
- Huang, H.; Qiao, X.; Chen, Z.; Chen, H.; Li, B.; Sun, Z.; Chen, M.; and Li, X. 2024. Crest: Cross-modal resonance through evidential deep learning for enhanced zero-shot learning. In *Proceedings of the 32nd ACM International Conference on Multimedia*, 5181–5190.
- Jing, L.; Parag, T.; Wu, Z.; Tian, Y.; and Wang, H. 2021. Videoss!l: Semi-supervised learning for video classification. In *Proceedings of the IEEE/CVF winter conference on applications of computer vision*, 1110–1119.
- Kuehne, H.; Jhuang, H.; Garrote, E.; Poggio, T.; and Serre, T. 2011. HMDB: A large video database for human motion recognition. In *2011 International Conference on Computer Vision*, 2556–2563.
- Kurakin, A.; Raffel, C.; Berthelot, D.; Cubuk, E. D.; Zhang, H.; Sohn, K.; and Carlini, N. 2020. Remixmatch: Semi-supervised learning with distribution matching and augmentation anchoring.
- Leong, M. C.; Tan, H. L.; Zhang, H.; Li, L.; Lin, F.; and Lim, J. H. 2021. Joint learning on the hierarchy representation for fine-grained human action recognition. In *2021 IEEE International Conference on Image Processing (ICIP)*, 1059–1063. IEEE.
- Leong, M. C.; Zhang, H.; Tan, H. L.; Li, L.; and Lim, J. H. 2022. Combined CNN transformer encoder for enhanced fine-grained human action recognition. *arXiv preprint arXiv:2208.01897*.
- Li, J.; Li, D.; Savarese, S.; and Hoi, S. 2023a. Blip-2: Bootstrapping language-image pre-training with frozen image encoders and large language models. In *International conference on machine learning*, 19730–19742. PMLR.
- Li, K.; He, Y.; Wang, Y.; Li, Y.; Wang, W.; Luo, P.; Wang, Y.; Wang, L.; and Qiao, Y. 2023b. Videochat: Chat-centric video understanding. *arXiv preprint arXiv:2305.06355*.
- Li, K.; Wang, Y.; He, Y.; Li, Y.; Wang, Y.; Liu, Y.; Wang, Z.; Xu, J.; Chen, G.; Luo, P.; et al. 2024. Mvbench: A comprehensive multi-modal video understanding benchmark. In *Proceedings of the IEEE/CVF Conference on Computer Vision and Pattern Recognition*, 22195–22206.
- Li, T.; Foo, L. G.; Ke, Q.; Rahmani, H.; Wang, A.; Wang, J.; and Liu, J. 2022. Dynamic spatio-temporal specialization learning for fine-grained action recognition. In *European Conference on Computer Vision*, 386–403. Springer.
- Li, Z.; He, L.; and Xu, H. 2022. Weakly-supervised temporal action detection for fine-grained videos with hierarchical atomic actions. In *European conference on computer vision*, 567–584. Springer.
- Lin, B.; Ye, Y.; Zhu, B.; Cui, J.; Ning, M.; Jin, P.; and Yuan, L. 2023. Video-llava: Learning united visual representation by alignment before projection. *arXiv preprint arXiv:2311.10122*.
- Ma, K.; Huang, H.; Chen, J.; Chen, H.; Ji, P.; Zang, X.; Fang, H.; Ban, C.; Sun, H.; Chen, M.; et al. 2024. Beyond uncertainty: Evidential deep learning for robust video temporal grounding. *arXiv preprint arXiv:2408.16272*.
- Mac, K.-N. C.; Joshi, D.; Yeh, R. A.; Xiong, J.; Feris, R. S.; and Do, M. N. 2019. Learning motion in feature space: Locally-consistent deformable convolution networks for fine-grained action detection. In *Proceedings of the IEEE/CVF International Conference on Computer Vision*, 6282–6291.
- OpenAI. 2024. GPT-4 System Card. <https://openai.com/index/gpt-4v-system-card/>. Accessed: 2024-08-03.
- Rizve, M. N.; Duarte, K.; Rawat, Y. S.; and Shah, M. 2021. In defense of pseudo-labeling: An uncertainty-aware pseudo-label selection framework for semi-supervised learning. *arXiv preprint arXiv:2101.06329*.
- Russakovsky, O.; Deng, J.; Su, H.; Krause, J.; Satheesh, S.; Ma, S.; Huang, Z.; Karpathy, A.; Khosla, A.; Bernstein, M.; et al. 2015. Imagenet large scale visual recognition challenge. *International journal of computer vision*, 115: 211–252.
- Shao, D.; Xiong, Y.; Zhao, Y.; Huang, Q.; Qiao, Y.; and Lin, D. 2018. Find and focus: Retrieve and localize video events with natural language queries. In *Proceedings of the European Conference on Computer Vision (ECCV)*, 200–216.
- Shao, D.; Zhao, Y.; Dai, B.; and Lin, D. 2020a. Finegym: A hierarchical video dataset for fine-grained action understanding. In *Proceedings of the IEEE/CVF conference on computer vision and pattern recognition*, 2616–2625.
- Shao, D.; Zhao, Y.; Dai, B.; and Lin, D. 2020b. Intra-and inter-action understanding via temporal action parsing. In *Proceedings of the IEEE/CVF Conference on Computer Vision and Pattern Recognition*, 730–739.
- Shu, W.-J.; Dou, H.-X.; Wen, R.; Wu, X.; and Deng, L.-J. 2024. CMT: Cross Modulation Transformer with Hybrid Loss for Pansharpening. *arXiv preprint arXiv:2404.01121*.
- Singh, A.; Chakraborty, O.; Varshney, A.; Panda, R.; Feris, R.; Saenko, K.; and Das, A. 2021. Semi-supervised action recognition with temporal contrastive learning. In *Proceedings of the IEEE/CVF Conference on Computer Vision and Pattern Recognition*, 10389–10399.
- Sohn, K.; Berthelot, D.; Carlini, N.; Zhang, Z.; Zhang, H.; Raffel, C. A.; Cubuk, E. D.; Kurakin, A.; and Li, C.-L. 2020. Fixmatch: Simplifying semi-supervised learning with consistency and confidence. *Advances in neural information processing systems*, 33: 596–608.
- Soomro, K. 2012. UCF101: A dataset of 101 human actions classes from videos in the wild. *arXiv preprint arXiv:1212.0402*.
- Tang, H.; Liu, J.; Yan, S.; Yan, R.; Li, Z.; and Tang, J. 2023. M3net: multi-view encoding, matching, and fusion for few-shot fine-grained action recognition. In *Proceedings of the 31st ACM international conference on multimedia*, 1719–1728.

- Tarvainen, A.; and Valpola, H. 2017. Mean teachers are better role models: Weight-averaged consistency targets improve semi-supervised deep learning results. *Advances in neural information processing systems*, 30.
- Tong, A.; Tang, C.; and Wang, W. 2023. Semi-Supervised Action Recognition From Temporal Augmentation Using Curriculum Learning. *IEEE Transactions on Circuits and Systems for Video Technology*, 33(3): 1305–1319.
- Tong, S.; Liu, Z.; Zhai, Y.; Ma, Y.; LeCun, Y.; and Xie, S. 2024. Eyes wide shut? exploring the visual shortcomings of multimodal llms. In *Proceedings of the IEEE/CVF Conference on Computer Vision and Pattern Recognition*, 9568–9578.
- Vemprala, S. H.; Bonatti, R.; Buckner, A.; and Kapoor, A. 2024. Chatgpt for robotics: Design principles and model abilities. *IEEE Access*.
- Wang, J.; Wang, Y.; Liu, S.; and Li, A. 2021. Few-shot fine-grained action recognition via bidirectional attention and contrastive meta-learning. In *Proceedings of the 29th ACM International Conference on Multimedia*, 582–591.
- Wang, L.; Xiong, Y.; Wang, Z.; Qiao, Y.; Lin, D.; Tang, X.; and Van Gool, L. 2016. Temporal segment networks: Towards good practices for deep action recognition. In *European conference on computer vision*, 20–36. Springer.
- Wang, L.; Xiong, Y.; Wang, Z.; Qiao, Y.; Lin, D.; Tang, X.; and Van Gool, L. 2018. Temporal segment networks for action recognition in videos. *IEEE transactions on pattern analysis and machine intelligence*, 41(11): 2740–2755.
- Wu, X.; Wu, X.; Luan, T.; Bai, Y.; Lai, Z.; and Yuan, J. 2024. FSC: Few-point Shape Completion. In *Proceedings of the IEEE/CVF Conference on Computer Vision and Pattern Recognition*, 26077–26087.
- Xiao, J.; Jing, L.; Zhang, L.; He, J.; She, Q.; Zhou, Z.; Yuille, A.; and Li, Y. 2022. Learning from temporal gradient for semi-supervised action recognition. In *Proceedings of the IEEE/CVF Conference on Computer Vision and Pattern Recognition*, 3252–3262.
- Xie, Q.; Dai, Z.; Hovy, E.; Luong, T.; and Le, Q. 2020. Un-supervised data augmentation for consistency training. *Advances in neural information processing systems*, 33: 6256–6268.
- Xing, Z.; Dai, Q.; Hu, H.; Chen, J.; Wu, Z.; and Jiang, Y.-G. 2023. Svformer: Semi-supervised video transformer for action recognition. In *Proceedings of the IEEE/CVF conference on computer vision and pattern recognition*, 18816–18826.
- Xiong, B.; Fan, H.; Grauman, K.; and Feichtenhofer, C. 2021. Multiview pseudo-labeling for semi-supervised learning from video. In *Proceedings of the IEEE/CVF international conference on computer vision*, 7209–7219.
- Xu, J.; Rao, Y.; Yu, X.; Chen, G.; Zhou, J.; and Lu, J. 2022a. Finediving: A fine-grained dataset for procedure-aware action quality assessment. In *Proceedings of the IEEE/CVF conference on computer vision and pattern recognition*, 2949–2958.
- Xu, Y.; Wei, F.; Sun, X.; Yang, C.; Shen, Y.; Dai, B.; Zhou, B.; and Lin, S. 2022b. Cross-model pseudo-labeling for semi-supervised action recognition. In *Proceedings of the IEEE/CVF Conference on Computer Vision and Pattern Recognition*, 2959–2968.
- Yan, Y.; Wang, S.; Huo, J.; Li, H.; Li, B.; Su, J.; Gao, X.; Zhang, Y.-F.; Xu, T.; Chu, Z.; et al. 2024a. Errorradar: Benchmarking complex mathematical reasoning of multi-modal large language models via error detection. *arXiv preprint arXiv:2410.04509*.
- Yan, Y.; Wen, H.; Zhong, S.; Chen, W.; Chen, H.; Wen, Q.; Zimmermann, R.; and Liang, Y. 2024b. Urbanclip: Learning text-enhanced urban region profiling with contrastive language-image pretraining from the web. In *Proceedings of the ACM on Web Conference 2024*, 4006–4017.
- Yang, C.; Xu, Y.; Shi, J.; Dai, B.; and Zhou, B. 2020. Temporal pyramid network for action recognition. In *Proceedings of the IEEE/CVF conference on computer vision and pattern recognition*, 591–600.
- Yuan, L.; Gundavarapu, N. B.; Zhao, L.; Zhou, H.; Cui, Y.; Jiang, L.; Yang, X.; Jia, M.; Weyand, T.; Friedman, L.; et al. 2023. Videoglue: Video general understanding evaluation of foundation models. *arXiv preprint arXiv:2307.03166*.
- Yun, S.; Han, D.; Oh, S. J.; Chun, S.; Choe, J.; and Yoo, Y. 2019. Cutmix: Regularization strategy to train strong classifiers with localizable features. In *Proceedings of the IEEE/CVF international conference on computer vision*, 6023–6032.
- Zhang, P.; Dong, X.; Zang, Y.; Cao, Y.; Qian, R.; Chen, L.; Guo, Q.; Duan, H.; Wang, B.; Ouyang, L.; Zhang, S.; Zhang, W.; Li, Y.; Gao, Y.; Sun, P.; Zhang, X.; Li, W.; Li, J.; Wang, W.; Yan, H.; He, C.; Zhang, X.; Chen, K.; Dai, J.; Qiao, Y.; Lin, D.; and Wang, J. 2024. InternLM-XComposer-2.5: A Versatile Large Vision Language Model Supporting Long-Contextual Input and Output. *arXiv preprint arXiv:2407.03320*.
- Zhao, L.; Gundavarapu, N. B.; Yuan, L.; Zhou, H.; Yan, S.; Sun, J. J.; Friedman, L.; Qian, R.; Weyand, T.; Zhao, Y.; et al. 2024. VideoPrism: A Foundational Visual Encoder for Video Understanding. *arXiv preprint arXiv:2402.13217*.
- Zheng, M.; Xu, Y.; Huang, H.; Ma, X.; Liu, Y.; Shu, W.; Pang, Y.; Tang, F.; Chen, Q.; Yang, H.; et al. 2024. VideoGen-of-Thought: A Collaborative Framework for Multi-Shot Video Generation. *arXiv preprint arXiv:2412.02259*.
- Zhou, B.; Andonian, A.; Oliva, A.; and Torralba, A. 2018. Temporal relational reasoning in videos. In *Proceedings of the European conference on computer vision (ECCV)*, 803–818.
- Zhu, X. J. 2005. Semi-supervised learning literature survey.
- Zou, Y.; Choi, J.; Wang, Q.; and Huang, J.-B. 2023. Learning representational invariances for data-efficient action recognition. *Computer Vision and Image Understanding*, 227: 103597.

## Appendix

### Introduction

The content of our Appendix is organized as follows:

- In Section A, we present the data processing employed in our SeFAR framework, as well as baseline analysis;
- In Section B, we expound upon the categorical analysis of model uncertainty;
- In Section C, we provide more discussions regarding our SeFAR;
- In Section D, we present detailed information regarding the newly built Gym-QA and Gym-New datasets.

### A. Data Processing and Baseline Analysis

**Data Processing.** In order to ensure a rigorous and equitable comparison, we adopt identical data processing procedures and input formats across both SeFAR and the baseline methods. It is noteworthy that the input data format utilized in our experiments may not be the same as the original versions presented in FineGym (Shao et al. 2020a) and FineDiving (Xu et al. 2022a) since we conduct experiments at the finest level within these two datasets. We release the data pre-processing scripts together with the whole project code for the convenience of future work.

**Baseline Analysis.** Semi-supervised fine-grained action recognition is a challenging task that has not been previously explored. This is evident from the experimental results (*e.g.*, Tab. 1), which show that models designed for coarse-grained action perform poorly on fine-grained actions. It is important to clarify that the baselines compared in Tab. 1 were evaluated and tested by us on the FineGym and FineDiving datasets for the first time, rather than by previous studies. The reason for including only three baselines in this comparison is that, although many studies have explored semi-supervised coarse-grained action recognition (*e.g.*, baselines in Tab. 2), only the three works presented in Tab. 1 are open-source and reproducible. We also attempted to reproduce models from non-open-source works based on their methodology sections, but unfortunately, the results we obtained differed from those reported in their original papers.

Notably, we have identified an impressive concurrent work, FinePseudo (Dave, Rizve, and Shah 2025), which is dedicated to addressing the problem of semi-supervised fine-grained action recognition. We will give it further attention and exploration in our future work.

### B. Visualization of Model Uncertainty

As highlighted by (Rizve et al. 2021), the escalation of uncertainty within model predictions inversely impacts the model’s reliability. A parallel phenomenon is discernible in our exploration of semi-supervised fine-grained action recognition. Specifically, we conducted a random sampling of 1000 data points from various datasets and employed the Teacher model to predict each set of 1000 data points, subsequently evaluating the accuracy of the Teacher model. The left panel of Fig. 5 illustrates the correlation between the confidence level associated with the Teacher model’s predictions and their corresponding accuracy; notably, predictions characterized by heightened confidence demonstrate

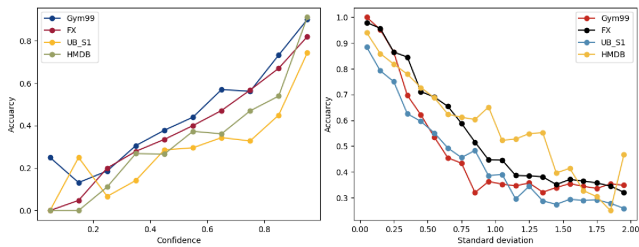


Figure 5: The relationship between the Teacher model’s prediction accuracy and its confidence (left), as well as its standard deviation (right).

augmented accuracy. Conversely, the right panel of Fig. 5 depicts the connection between the standard deviation of predictions generated by the Teacher model and their accuracy; a diminished variance in predictions is concomitant with heightened accuracy. This visual representation corroborates the rationale underpinning our conceptualization of the *Adaptive Regulation*.

### C. More Discussions on SeFAR

In this section, we further discuss the following research questions ( $RQ$ ):

- $RQ1$ : How does each module contribute to enhancing fine-grained action recognition?
- $RQ2$ : How does the *dual-level temporal elements modeling* differ from previous modeling strategies?
- $RQ3$ : Will the *moderate temporal perturbation* alter the actions?
- $RQ4$ : Can the *adaptive regulation* be effective under more challenging conditions?
- $RQ5$ : Does the teacher model’s prediction frequency affect performance?
- $RQ6$ : What are the limitations of the current approach, and what directions should future research take?

**Module Analysis of SeFAR ( $RQ1$ ):** ① *Dual-level temporal elements modeling*: As discussed earlier, fine-grained actions, compared to coarse-grained actions, not only rely heavily on global semantic context but also contain richer visual detail, presenting unique challenges. The dual-level temporal elements we designed divide a video into two hierarchical levels (*i.e.*, fine-grained elements  $p_i$ , and context element  $p^{\text{context}}$ ). This provides multi-granular information for fine-grained action recognition, allowing the model to capture features at different temporal scales (*e.g.*, varying numbers of giant swings), and offering diverse representations for actions of different durations. ② *Moderate temporal perturbation*: In semi-supervised learning, data augmentation is essential for consistency regularization, which leads to more stable and superior model performance. Traditional coarse-grained action recognition often uses spatial augmentations that may disrupt critical details needed for fine-grained actions. For example, while coarse-grained actions like “running” can be recognized even with masked frames, fine-grained actions are characterized by complexity and coherence. Therefore, we focus on temporal augmentations in this

Table 6: **Ablation of different labeling rates.** The first two raw demonstrate our SeFAR w/o and w/ the Adaptive Regulation (Ada-Reg) respectively. The third raw further shows the performance increase rates at different labeling rates.

Method	FineDiving				
	1%	3%	5%	7%	10%
SeFAR w/o Ada-Reg	61.5	64.6	67.2	69.7	73.4
SeFAR	<b>66.3</b>	<b>69.5</b>	<b>72.2</b>	<b>74.6</b>	<b>78.4</b>
Increase (%)	7.8%↑	7.6%↑	7.4%↑	7.0%↑	6.8%↑

Table 7: Deeper comparison of temporal augmentations.

Perturbation	Speed/Order	FX	10m	UB-S1	5253B
Slow-rate	Speed	22.4	81.2	35.6	92.8
T-Drop	Speed	22.4	81.2	35.6	92.8
All shuffle	Order	23.5	82.8	36.1	93.5
Local-shuffle	Order	23.0	84.1	36.5	94.9
Warping	Order	23.4	81.9	34.7	92.9
T-Half	Order	23.3	83.0	35.3	93.4
All reverse	Order	23.6	83.7	35.5	95.1
Mod-Perturb	Order	<b>23.8</b>	<b>85.5</b>	<b>36.6</b>	<b>96.4</b>

work. As shown in Tab. 4, excessive perturbations can disrupt sequence information, hindering the model’s ability to capture subtle action differences. Our experiments show that sequence reversal provides strong perturbations while preserving action continuity, making them more effective for temporal augmentation. Additionally, our moderate temporal perturbation retains global context, enabling the model to benefit from augmentation while maintaining a coherent understanding of actions. **Adaptive regulation:** In fine-grained action recognition, subtle differences between similar actions (*e.g.*, examples in Fig. 1) can lead to significant fluctuations in the predictions made by the Teacher model, particularly in a semi-supervised setting, as illustrated in Fig. 4. The adaptive regulation strategy plays a crucial role in stabilizing the training process by automatically adjusting the weights of the loss functions based on the distribution of the Teacher model’s predictions, which is essential for effective semi-supervised fine-grained action recognition.

**Dual-level Temporal Elements Modeling (RQ2):** Sampling at different temporal scales is actually not a new approach in action recognition. However, unlike previous methods, *e.g.*, TPN (Yang et al. 2020)), which model at the *feature* level and sample once at each level, following an “ $L^1 < L^2 \dots < L^N$ ” hierarchy for an N-level pyramid, often leading to high frame sampling and computational demands, our dual-level temporal elements modeling represents different video speeds through multi-level sampling at the input stage. We employ multiple fine-grained elements, each with the same number of frames (*i.e.*, 2), and a single context element to capture local and global features, respectively. This design allows us to achieve better performance while minimizing the total number of sampled frames.

To achieve a deeper comparison with other temporal perturbations, we assessed each method on sub-tasks involving the recognition of elements with an event (FX, 10m)

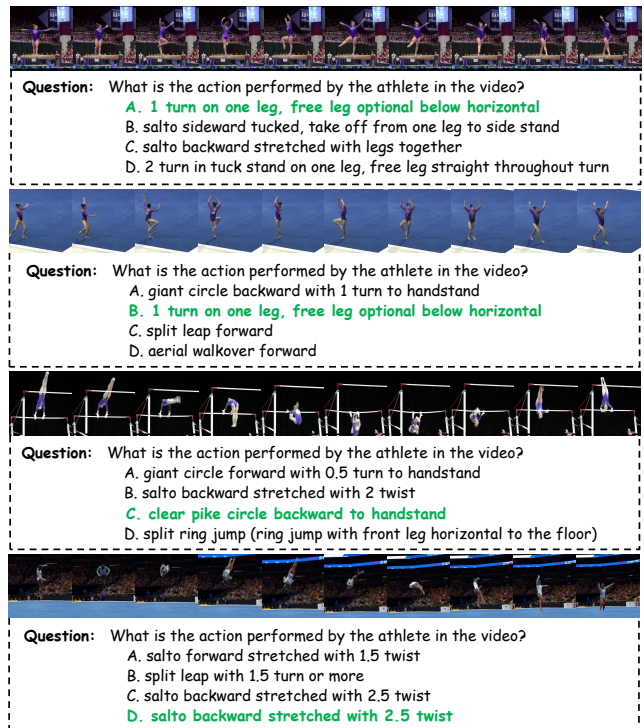


Figure 6: Examples of Gym-QA

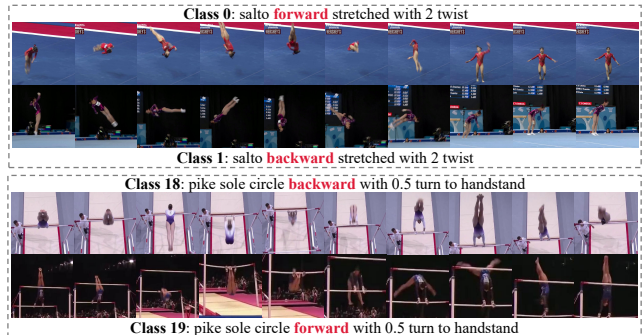


Figure 7: Examples of Gym-New

and within a set (UB-S1, 5253B) using 10% labeled data as shown in Tab. 7. Consistent with the results in the main text (Tab. 4), our proposed moderate temporal perturbation (Mod-Perturb) consistently outperformed all other strategies across all sub-tasks, demonstrating its superior efficacy.

**Potential Action Directionality Changes (RQ3):** Human actions are inherently complex to a certain extent (Shao et al. 2018, 2020b). Intuitively, the reversal of action videos introduces challenges related to the directionality of actions (*e.g.*, “sitting down” vs. “standing up”). We have taken this into account in our dual-level temporal elements modeling design, which includes both fine-grained elements containing local details and context elements capturing global information. During temporal perturbation, we only reverse the fine-grained elements, preserving the original temporal order in the context elements. This allows us to achieve consistency regularization through temporal perturbation while maintaining the original global temporal structure, which



Figure 8: Confusion matrix of baseline (left) and ours (right) on Gym-New 10%, where the horizontal coordinate represents the predicted label and the vertical coordinate represents the true label. The labels corresponding to actions are shown in Fig. 9.

differs significantly from complete reversal and previous temporal augmentation methods applied at the video level. This also indicates that our dual-level temporal elements modeling is coupled with moderate temporal perturbation, rather than being a simple modular combination. Furthermore, as demonstrated in Tab. 4, we validated this approach by constructing a variant of the FineGym dataset composed of completely *opposite action pairs*, named Gym-New, for experimentation. The results further confirm that for fine-grained action recognition tasks, which require temporal and spatial coherence, common temporal augmentation strategies may disrupt this coherence, whereas our moderate temporal perturbation maintains coherence while introducing significant temporal disturbance.

**Adaptive Regulation (RQ4):** With the continuous advancement of deep learning (Chen et al. 2024a; Yan et al. 2024b; Chen et al. 2024b; Ma et al. 2024; Huang et al. 2024; Yan et al. 2024a; Shu et al. 2024; Wu et al. 2024), the data-hungry paradigm of fully supervised learning has increasingly revealed certain limitations. Unlike the extensively studied fully-supervised setting, semi-supervised learning typically operates with a label rate ranging from 1% to 10%, making it particularly suitable for tasks like fine-grained action recognition that require high-quality data. However, low label rates can lead to instability during training, as discussed in the main text. To address this challenge, we designed the Adaptive Regulation process. In a semi-supervised setting, lower label rates present greater difficulties. Therefore, to further explore the potential of our strategy, we conducted experiments under varying label rates, as shown in Tab. 6. The results demonstrate that as the label rate decreases, the performance enhancement provided

Table 8: Computation analysis of teacher model predictions. Time shown in (ms).

Prediction Times	1	2	5	10	15	20
Teacher time / Iter.	29.9	68.5	75.8	160.4	260.1	361.3
Total time / Iter.	982.8	991.6	1005.1	1080.7	1220.6	1417.6
Portion (%)	3.0	6.9	7.5	14.8	21.3	25.5
Accuracy (%)	-	35.3	36.2	36.7	36.8	37.0

by adaptive regulation becomes more pronounced, further validating that our strategy can effectively maintain strong performance under more challenging conditions.

**Efficiency of Teacher Model Prediction (RQ5):** During inference, only the student model is used, incurring no additional computational cost from the teacher model. In the training phase, as shown in Tab. 8, we conduct further analysis focusing on ① *Time Cost*: Teacher prediction time increases with more predicted but remains a small fraction of total training time (e.g., 14.8% at 10 predictions). This efficiency is achieved as teacher predictions are parallelized and do not involve gradient computations. ② *Accuracy Impact*: Model accuracy improves with the number of predictions, tending to saturate around 10 predictions. Therefore, we set the number of teacher predictions to 10 to balance performance and computational efficiency.

**Limitation and Future Work (RQ6):** In this work, we introduce SeFAR to address the challenging task of semi-supervised fine-grained action recognition for the first time, achieving superior performance with the aid of our carefully designed modules. This advancement establishes a robust baseline for future research. However, one limitation of this

FX	Floor Exercise	BB	Balance Beam	UB	Uneven Bars		
0	salto forward stretched with 2 twist	8	salto forward tucked with 1 twist	18	pike sole circle backward with 0.5 turn to handstand	29	clear hip circle forward to handstand
1	salto backward stretched with 2 twist	9	salto backward tucked with 1 twist	19	pike sole circle forward with 0.5 turn to handstand	30	clear pike circle backward to handstand
2	salto forward stretched with 1 twist	10	salto forward tucked	20	giant circle backward with 1.5 turn to handstand	31	clear pike circle forward to handstand
3	salto backward stretched with 1 twist	11	salto backward tucked	21	giant circle forward with 1.5 turn to handstand	32	stalder backward with 0.5 turn to handstand
4	salto forward stretched with 1.5 twist	12	salto forward stretched with 1.5 twist	22	giant circle backward with 1 turn to handstand	33	stalder forward with 0.5 turn to handstand
5	salto backward stretched with 1.5 twist	13	salto backward stretched with 1.5 twist	23	giant circle forward with 1 turn to handstand	34	stalder backward to handstand
6	salto forward stretched with 0.5 twist	14	salto forward stretched with 1 twist	24	giant circle backward	35	stalder forward to handstand
7	salto backward stretched with 0.5 twist	15	salto backward stretched with 1 twist	25	giant circle forward	36	transition flight from high bar to low bar
		16	salto forward stretched	26	clear hip circle backward with 0.5 turn to handstand	37	transition flight from low bar to high bar
		17	salto backward stretched	27	clear hip circle forward with 0.5 turn to handstand	38	(swing forward) double salto backward tucked
				28	clear hip circle backward to handstand	39	(swing backward) double salto forward tucked

Figure 9: Labels corresponding to actions in Gym-New.

study is that we focused on temporal augmentation to emphasize its importance in fine-grained action understanding, while neglecting further exploration of spatial augmentation. We plan to address this in future work.

Another potential limitation is that our core modules rely solely on RGB video input, overlooking the contribution of multimodal information in visual tasks. While we acknowledge that multimodal inputs, *e.g.*, pose and textual descriptions, can significantly enhance model performance, we think that for the specific task of fine-grained action recognition—where data collection and annotation are particularly challenging—relying on such inputs could limit the model’s generalizability. Moreover, the extraction and annotation of fine-grained action-related pose and textual descriptions pose significant challenges due to their complex nature and the domain-specific knowledge required.

With the advancement of generative models (Chen et al. 2024c; Zheng et al. 2024), we will strive to overcome these limitations in future work and further explore advanced models’ fine-grained visual understanding and generation capabilities.

#### D. Gym-QA and Gym-New

**Gym-QA.** To facilitate the evaluation of MLLMs in fine-grained action understanding, we adapted the FineGym dataset into a multiple-choice format, creating the Gym-QA dataset, as illustrated in Fig. 6. Following the coarse-grained action recognition paradigm from VideoChat2 (Li et al. 2024), we posed the question: “What action is the athlete performing in the video?” The answer options included one correct label and three distractor labels from the FineGym dataset.

**Gym-New.** As demonstrated in Fig. 7, the Gym-New dataset is created by selecting direction-opposite action pairs from FineGym. This aims to provide a more challenging environment for fine-grained action understanding, further testing the temporal perturbation that is the focus of our work.

To delve deeper into the temporal directionality of ac-

tions, as illustrated in Fig. 8, we present the confusion matrices of our baseline, namely SVFormer (Xing et al. 2023) (Left), and our proposed SeFAR (Right) applied to FineGym-New dataset. Our method capitalizes on *dual-level temporal elements modeling*, which yields diverse temporal features, and *moderate temporal perturbation*, which enhances the model’s focus on temporal feature modeling. This leads to two notable improvements over the baseline: **a)** Our method effectively mitigates the impact of class imbalance, manifesting in a significant increase in the accuracy of under-represented classes; **b)** Our approach minimizes confusion between actions with opposing temporal directions (*e.g.*, “*forward*” vs. “*backward*”), while also reducing confusion among similar actions, *e.g.*, “*giant circle backward with 1 turn to handstand*” vs. “*giant circle backward*”.